EXTRACTION OF SEABED GEOMORPHOLOGIC FEATURES OF SVALBARD FJORDS USING HIGH-RESOLUTION SIDE SCAN SONAR

JAROSŁAW TĘGOWSKI[a], JERZY GIŻEJEWSKI[b], ADAM ZIELINSKI[c]

[a]Institute of Oceanology, Polish Academy of Sciences
Powstancow Warszawy 55, 81-712 Sopot, Poland
tegowski@iopan.gda.pl

[b]Institute of Geophysics, Polish Academy of Sciences
Ks. Janusza 64, 01-452 Warsaw, Poland
gizej@igf.edu.pl

[c]University of Victoria, Department of Electrical and Computer Engineering
P.O. Box 3055, Victoria, B.C., Canada V8W 3P6
Adam.Zielinski@ece.UVic.CA

This paper presents results of a study on the relationship between features of side scan sonar acoustic imagery of zones with active bedforms and geomorphologic seafloor characteristics. Acoustic measurements were conducted in Hornsund, a Svalbard fjord representing a periglacial environment with great intensity of morphodynamic processes and rapidly progressing changes of tidewater glaciers. Due to the intensity of these processes, Arctic fjords are the most promising areas to study the effects of climate change on the ecosystem. Acoustic identification of sedimentary structures and morphological forms created by currents and iceberg transport of glacier sediment away from the ice margin was performed. The spectral and fractal features of the recorded signals were analysed. The proposed analysis scheme allows identification of the morphodynamic active zones in the changing Arctic fjord environments. Measurements of acoustical features of seafloor surface were made during the 2006 Arctic cruise of r/v Oceania.

INTRODUCTION

Global warming induces climate changes, which are particularly visible in the Arctic environment. A long series of observations of Hornsund fjord glaciers (on Spitsbergen Island,

off the Svalbard Archipelago of Norway [Figure 1]) has shown that environmental changes in this area can be considered representative for the Atlantic sector of the Arctic. For that reason, the Hornsund fjord can be treated as a natural and representative laboratory, and results of research in this area are of great significance for monitoring and predicting global warming trends.Side scan sonar gives a very high resolution of the acoustic response of the seafloor and has been shown to be a useful tool for recognizing sedimentary environments. The intensity of sound backscattered from features of the bottom surface provides information about characteristics of the seafloor morphology. This tool is especially helpful in recognition of the bottom morphology of the Arctic periglacial environment, where traces of melting glaciers are visible in the seabed surface.

The main purpose of this paper is to outline a fast and comprehensive method to ascertain the essential morphological feature of the bottom surface: its degree of roughness (corrugation). Our method provides the fractal dimension as a measure of surface roughness [1]. The idea of using fractal dimensions for seafloor characterization is based on the assumption that a bottom surface has a fractal structure that can be transferred onto the shape of the acoustic echo during scattering [2]. That a bottom surface has different scales of surface roughness determines the fractality of the echo shape and, therefore, determines the fractality of side scan sonar bottom imagery.

1. MORPHOLOGY OF HORNSUND FJORD

The large fjords of Spitsbergen are grouped along the western coast. Their course is normally latitudinal, perpendicular to the coast. Vijdefjorden fjord is an exception; it runs longitudinally, with its mouth in the north of Spitsbergen island, and is genetically linked to the giant tectonic zone called the Billefjorden Fault Zone [6]. The tectonic layout of latitudinal fjords is not as obvious as that of the longitudinal, and for Hornsund these are only

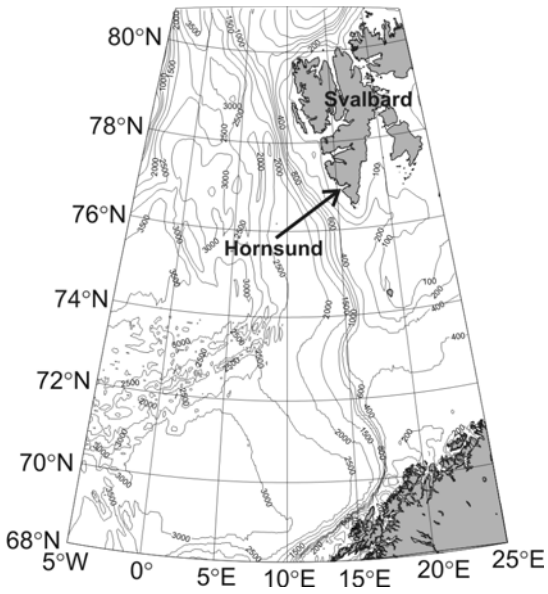

Fig.1 Map of Svalbard Archipelago and location of Hornsund fjord

suggestions [7]. The fjords are probably periglacial or interglacial river valleys [6], remodelled by glacial processes. Ice streams on the Isfjorden fjord and Van Mijenfjorden fjord are distinguished in the Weichselian Barents Sea ice-sheet [8]. The existence of a similar stream on Hornsund seems probable, suggested by the roughly linear, latitudinal course of the fjord axis and the funnel-like shape widening to the west [Figure 2]. Narrowing is due to longitudinally situated mountain ranges separated by the valleys of side glaciers. Visibly overdeepened basins on the fjord bottom are found in its central part, with smaller ones in the area near the mouth and the end section (Brepolen). The sills separating the basins run longitudinally. Overdeepening (basins) also occurs in the valleys of side-glaciers of Samarinvagen and Burgerbukta.

Over the past few decades, the glacier fronts in Hornsund have been retreating rapidly [9]. This has left the most distinctive mark in the eastern part of the fjord (Brepolen), where the glacier fronts have changed their position by about 5 to 7 km in the last 50 years. Bathymetric measurements conducted in the eastern part of the fjord in 2007 (Moskalik, oral information) suggest that the axis of the main glacier valley runs the same way as the Horn glacier axis, towards the eastern coast. Radar profiling [9] has not shown with full certainty that the bottom of this valley lies below sea level; however, the flow of the glacier from the Barents Sea ice-sheet was easier here than in fjords farther to the north that are enclosed from the east by mountain ranges. Thanks to these observations, we have more evidence that an ice stream exists in the Weichselian Barents Sea ice-sheet, flowing in the same direction as the Hornsund fjord's axis. Apart from the fjord's bottom morphology, the existence of a glacial lobe protruding onto the shelf in the fjord's forefield is also suggested by seismoacoustic studies documenting the presence of a large cone with recessional moraines on the surface [10].

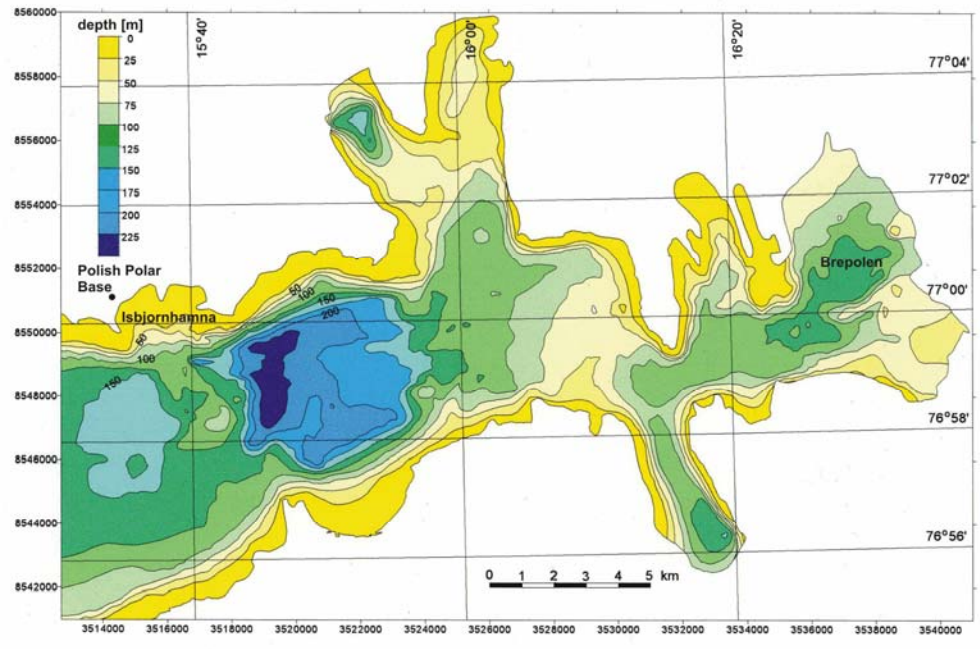

Fig.2 Bathymetric map of Hornsund fjord

Hornsund has been the object of intensive research since the late 19th century, but the primary focus of observation has been processes occurring on land. Extensive bathymetric measurements were carried out by the ships of successive expeditions of the Institute of Geophysics, Polish Academy of Sciences, and during the second geodynamic marine expedition to the Spitsbergen Archipelago region in 1985 [11]. A bathymetric map (Figure 2) was developed on their basis, as part of a topographic map at a scale of 1: 25,000 [11]. This map was used for editing all subsequent derivative maps.

Ever since the Polish Polar Station was built (1956/57), and especially since it opened as a year-round research station (1978/79), the intensity of research in the fjord region has increased substantially. The Hans glacier and its forefield is the object of model-oriented research. Isbjornhamna, the bay into whose eastern part the Hans glacier flows, has been the object of several bathymetric studies [12, 13, 14, 15, 16].

The Isbjornhamna bay is distinctly divided into two parts: the western part between the Wilczek and Baranowski peninsulas is shallow, and the bottom is a strandflat cut in the metamorphic rock of the Hecla Hoek formation. The sediments on the strandflat are residual, discontinuous, composed of sand and gravel deposits with larger rock debris and a small addition of fine-grained sediment. The entire bottom in this part of the bay is situated above the base of storm waves, so successive greater storms on the Greenland Sea cause significant changes to the sediment covering. The strandflat ends in a distinct edge from which the bottom's surface slopes down towards the overdeepening of the fjord, exceeding a depth of 150 m.

The eastern part of the bay between the Baranowski and Oceanographer peninsulas is enclosed by a distinct sill about 20 m deep, stretching between the tips of the two peninsulas. Between this sill and the current glacier front, a visible overdeepening of the bottom exceeds 150 m in depth. The eastern part of the sill on the edge of the slope going down into the fjord is covered with sand and gravel sediments displaying clear signs of rhythmic transport by waves reaching the bottom. Images of the bottom obtained from side scan sonar show the presence of sediment structures in the form of asymmetric wave streaks whose asymmetry suggests a direction of shift towards the glacier.

In a cross-section parallel to the glacier front, the area of the overdeepening is distinctly dual. The eastern part is shallower and less diverse morphologically. The bottom slopes gently towards the valley axis, forming a terrace surface restricted by a clear edge at a depth between 25 m and 30 m. The deep part of the valley has a bottom divided into a number of irregular basins restricted by ridges, probably of recessional moraines, ranging from several to almost twenty meters in height. The hollows are filled to varying degrees with sediments (silt, mud, diamicton) with locally present rock debris of larger dimensions (dropstones). The sediments are diverse and include numerous traces of the presence of benthic organisms as well as synsedimentational or postsedimentational disturbances in the form of flow stratification or layering with unstable density gradients.

2. FRACTAL DIMENSION OF SIDE SCAN IMAGERY OF BOTTOM SURFACE

The Hausdorff (fractal) dimension, D_H, of such structure is defined as [3, 4]:

$$D_{\mathrm{H}} = \lim_{r \to 0} \frac{-\log_{10} N(r)}{\log_{10} r}, \tag{3.1}$$

where $N(r)$ is the smallest number of open balls $B(p, r)$ with centre p and radius r needed for complete coverage of the object. $B(p, r) = \{x: \text{dist}(x, p) < r\}$, where dist$(x, p)$ is the distance between the point x and p. The fractal structure of the fractal dimension is described by a power rule, where the fractal dimension occurs as an exponent [3]:

$$N(r) = C_D \cdot \left(\frac{1}{r}\right)^{D_H}, \tag{3.2}$$

and where C_D is a constant. The fractal dimension of two-dimensional objects (e.g., curves) ranges from 1 to 2; of surfaces, from 2 to 3. A low value of fractal dimension corresponds to objects with uncomplicated shapes, while higher values are consistent with more complicated, irregular structures. To form an estimation of the Hausdorff dimension of an object directly from equation 1.1 is practically impossible; it is typically calculated using equivalent methods. From among many techniques of fractal dimension estimation (e.g., [5]), for our analysis of acoustical signals scattered by the sea bottom surface and registered by side scan sonar, we chose a method based on features of the spectral power density of the echo signal.

The power spectral density of an acoustical echo signal (A-scan – one echo line of side scan sonar imagery of sea bottom surface contains information about the complexity of the scattering medium. [1. where does parenthesis end? 2. remove parenthesis entirely and place information in a full sentence at the beginning] For a time interval $0 \le t \le T$, the Fourier transformation, $X(f,T)$, of an echo signal $x(t)$ of frequency f is:

$$X(f,T) = \int_0^T x(t) \mathrm{e}^{-2\pi i f} \, dt \,. \tag{3.3}$$

The result of the transformation is the power spectral density, $S(f)$, of the A-scan signal in the frequency domain:

$$S(f) = \frac{1}{T} |X(f,T)|^2 \,. \tag{3.4}$$

If $x(t)$ has fractal features, then the relationship between the power spectral density and frequency will satisfy a power rule for a certain frequency interval Δf:

$$S(f) = \frac{1}{T} K_D \cdot f^{-\beta}, \tag{3.5}$$

where K_D is a constant and β is the exponent of the power function that determines the value of the fractal dimension. As Mandelbrot (1982) has shown, the fractal dimension D_{FFT} is related to the signal spectrum:

$$D_{FFT} = \frac{5 - \beta}{2}, \tag{3.6}$$

where β is the slope of the regression line of the power spectral density function. Figure 3 shows an example of fractal dimension computation, where the slope of $S(f)$ determines D_{FFT} (equation 3.6).

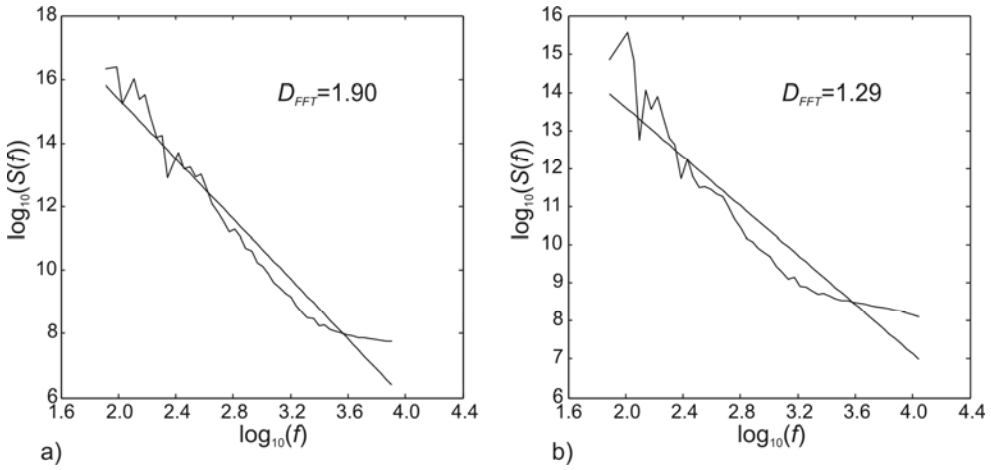

Fig.3 Determination of fractal dimension from slope of power spectral density function in the log-log scale, where a) D_{FFT}=1.90, b) D_{FFT}=1.29

3. DATA AQUISITION AND PROCESSING

The recording of acoustical signals scattered at the bottom surface of Hornsund fjord was conducted using an EdgeTech DF-1000 side scan sonar operating at 100 kHz and 390 kHz. The sonar fish was towed from the r/v Oceania in her 2006 Arctic cruise (Figure 4). During

Fig.4 Side scan sonar transects in Hornsund fjord

the measurements, operators of acoustical equipment kept a constant distance between the seafloor and the towed acoustical transducer system, because it was significant for the preservation of horizontal and vertical scales of irregularities of seafloor surfaces registered in the form of side scan sonar images. Acoustical transects were mainly conducted perpendicularly to the Hans glacier front. The locations and distances between transects were limited by occurrence of underwater rocks in the shallow water areas of Isbjornhamna. Additional measurement limitations came from drifting icebergs and oceanic long wave swell resulting in variation of ship courses. An illustration of r/v Oceania side scan sonar transects in Hornsund fjord is presented in a topographic map, Figure 4, where four almost parallel transects are marked.

In the shallow areas located close to the glacier front (see Figure 2 and 4) the surface of the seafloor bottom is corrugated as the result of icebergs scraping the bottom. The depth of iceberg footprints exceeds 40 meters. An example of such form of irregular seafloor surface is shown in Figure 4, where parallel furrows in the sandy and gravelly bottom are visible. Figure 5 depicts a different seafloor surface pattern from a deep part of the fjord. Bioturbed sediments (mud, silt, and clay) create a flat basin bottom containing signs of biological benthic habitats and stones or pebbles coming from melting icebergs. As the measure of seafloor surface corrugation, we applied the fractal dimension calculated as described in section 3. The estimation of the D_{FFT} parameter required several steps. In the first step, we divided the side scan sonar registration for parts containing 1000 A-scans. For bottom images

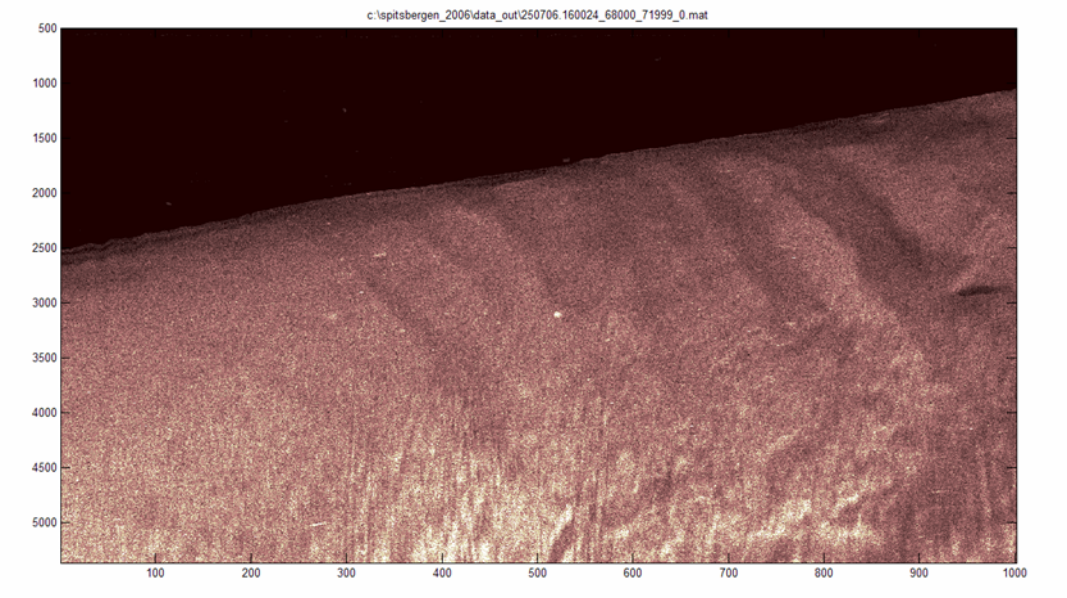

Fig.5 Side scan sonar image (100 kHz) of corrugated bottom located close to the glacier front

prepared this way (e.g., Figures 5 and 6), the sections of water body registration were rejected and centers of the clipped images were found. In the next step, 24 (every 15 degrees) cross sections containing the centers of images were chosen. For each cross section, the fractal dimension D_{FFT} was estimated. Examples of the results of this procedure for two sections of side scan sonar bottom imagery (Figures 5 and 6) are presented in Figure 7, where circular plots show values of D_{FFT} parameters for 24 chosen directions. Finally, mean values were calculated. The mean value of D_{FFT} for the case of a corrugated surface is 1.90 (Figure 7.a) and for a flat surface is 1.29 (Figure 7.b).

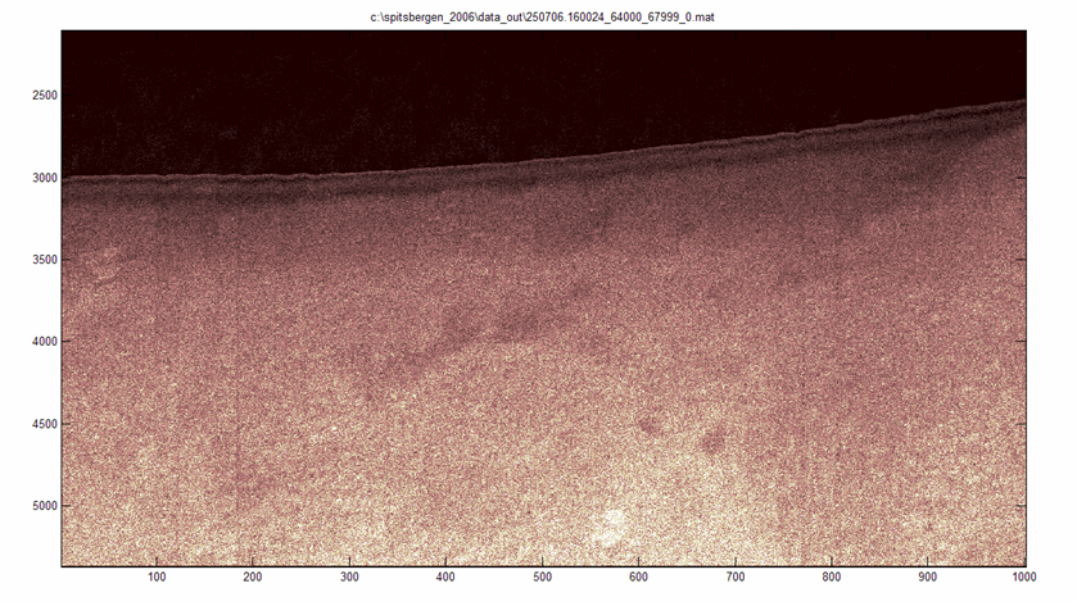

Fig.6 Side scan sonar image (100 kHz) of flat bottom in the deep part of the Hornsund fjord

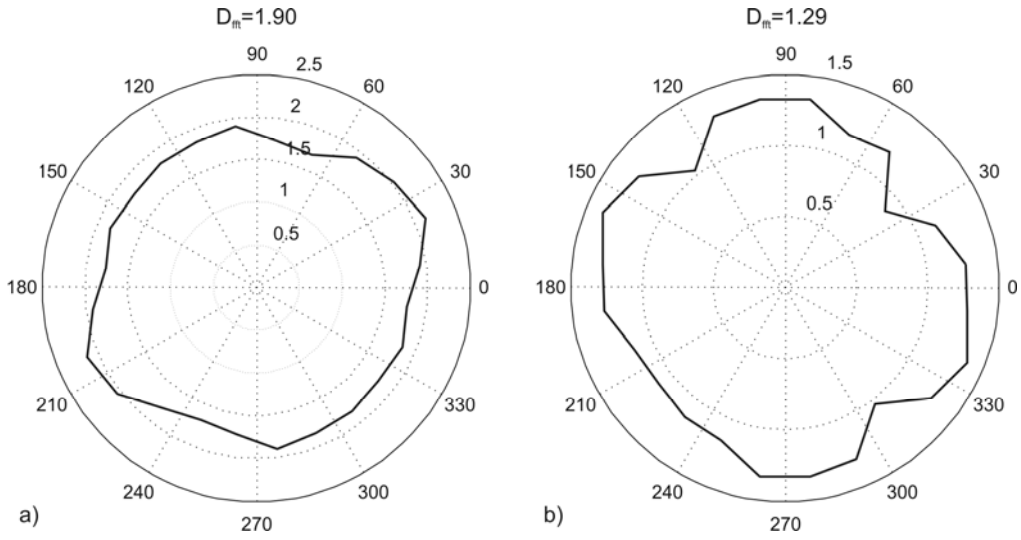

Fig.7 Circular plots of fractal dimension calculated for side scan sonar seafloor interceptions, where a) mean D_{FFT}=1.90 (surface from Figure 5) and b) mean D_{FFT}=1.90 (surface from Figure 6)

Figure 8 shows the result of fractal dimension estimation for the experimental area (see map of transects in Figure 4). Black circles depict mean values of fractal dimension in the measured areas. The biggest values of the D_{FFT} parameter are found in the part of the fjord where icebergs influence the bottom shape, while the smaller are characteristic of flat, deeper areas.

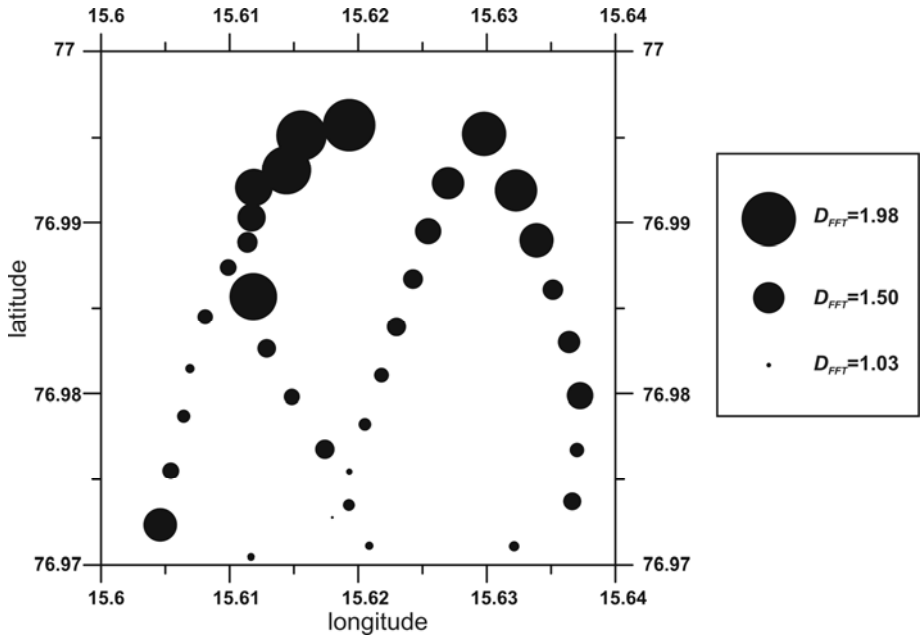

Fig.8 Estimated values of fractal dimension for the experiment area (see map in Figure 3)

4. CONCLUSIONS

The side scan sonar image parameterization presented in this study has many promising features that allow determination of the morphological forms of the seabed. The presented technique of calculation of the seafloor fractal dimension gave satisfactory results in the complex and diversified Arctic fjord environment. The proposed method allows for rapid estimation of seafloor corrugation, which is helpful for benthic habitat description.

ACKNOWLEDGEMENTS

This work was supported by the Ministry of Education and Science of Poland (research project no. 3 P04E 005 25).

REFERENCES

1. J.A Ogilvy, *Theory of wave scattering from rough surfaces*. Adam Hilger, 277, Bristol 1991.
2. T. Yamamoto, *Acoustic scattering in the ocean from velocity and density fluctuations in the sediments*, Journ. Acoust. Soc. Am. 99 (2), 866-879, 1996.
3. B.B. Mandelbrot, *The fractal geometry of nature*, Freeman, pp.480, San Francisco 1982.
4. H.M. Hastings, G. Sugihara, *Fractals, A user's guide for the natural sciences*, Oxford University Press, pp. 248, Oxford 1996.
5. J. Schmittbuhl, J. P. Vilotte, S. Roux, *Reliability of self-affine measurements*, Phys. Rev. E 51, 131-147, 1995.
6. B.W. Harland, *The geology of Svalbard*. Geological Society Memoir No. 17, pp. 521, 1997.

7. J.Bednarek, S. Rudowski, S.M. Zalewski, The tectonic scetch of the offshore area within Hornsund region, Spitsbergen, In Repelewska-Pękalowa, J., Pękala, K. (eds), XX Polar Symposium, *Man's Impact on the Polar Environment*, June 3-5, 293-297, Lublin 1993.
8. C.R. Stokes, C.D. Clark, Palaeo-ice streams, *Quaternary Science Reviews* No 20, 1437-1457, 2001.
9. J. Jania, P. Głowacki, E. Bukowska-Jania, L. Kolondra, Z .Perski, M. Pulina, A.M. Piechota, J. Szafraniec, W. Dobiński, B.A. Piwowar, Lodowce otoczenia Hornsundu. In: Kostrzewskui, A., Pulina, M., Zwoliński, Z. (eds), *Warsztaty Glacjologiczne Spitsbergen*, 68-98, 2004.
10. A. Marsz, *Rzeźba szelfu zachodniego wybrzeża Spitsbergenu w rejonie przylegającym do Hornsundu*. Przegląd Geograf. 64 (1-2), 137-145, 1993.
11. S. Barna, Z. Warchoł, *Spitsbergen, Hornsund, Mapa topograficzna 1:25 000*, Wojskowe Zakłady Kartograficzne, Warszawa 1987.
12. R. Siwecki, S. Swerpel, J. Urbański, *Batymetria Zatoki Białego Niedźwiedzia*. In: V Sympozjum Polarne, Gdańsk – Gdynia 28-29 kwietnia, 124-128, 1978.
13. W. Moskal, unpublished, *Charakterystyka hydrologiczna Zatoki Białego Niedźwiedzia (Spitsbergen)* - praca magisterska, Instytut Oceanografii Uniwersytetu Gdańskiego, pp. 78, Gdynia 1987.
14. J. Różański, unpublished, *Locja Hornsundu na Spitsbergenie, Poradnik dla statków udających , się do Polskiej Stacji Polarnej w Hornsundzie*, NAVIGA, Gdynia 1989.
15. J. Giżejewski, *Bottom morphology of the Hans Glacier forefield (Hornsund, South-West Spitsbergen, Svalbard). Preliminary report*. In P. Głowacki (ed), Polish Polar Studies, 24th Polar Symposium, Warszawa 1997, 63-67, 1997.
16. J. Giżejewski, A. Kruss, J. Tęgowski, J.M. Węsławski, unpublished, *Wielkoskalowy model zmienności i różnorodności młodego środowiska peryglacjalno – morskiego Zatoki Białego Niedźwiedzia (Spitsbergen, Hornsund)*. Projekt N. 3 P04E 005 25, Raport Końcowy, część merytoryczna, 2007.